EUROPEAN JOURNAL OF CANCER 47 (2011) 1420–1431

available at www.sciencedirect.com

ScienceDirect

journal homepage: www.ejconline.com

Phosphoprotein pathway profiling of ovarian carcinoma for the identification of potential new targets for therapy

Dana Faratian *, *InHwa Um, Danielle S. Wilson, Peter Mullen, Simon P. Langdon, David J. Harrison*

Division of Pathology & Edinburgh Breakthrough Research Unit, Institute of Genetics and Molecular Medicine, University of Edinburgh, Crewe Road South, Edinburgh EH4 2XU, Scotland, UK

ARTICLE INFO

Article history:
Received 18 October 2010
Received in revised form 26 December 2010
Accepted 20 January 2011
Available online 18 February 2011

Keywords:
Ovarian cancer
Immunofluorescence
Cytotoxic chemotherapy
Patient-tailored therapy
Molecular classification
Targeted therapy

ABSTRACT

Advances in predicting responses to therapies in ovarian cancer have not matched progress seen in other solid-organ tumours: ovarian cancer remains a poor-prognosis disease. There has been a paradigm shift in molecular therapeutics away from targeting individual molecules to whole biological pathways. The aim of this study was to quantitatively measure the activation state of druggable oncogenic pathways by generating a phosphoprotein profile in cancer tissues, in order to establish associations with clinicopathological parameters and to identify treatment groups for targeted therapy. In total we analysed the expression of ten phosphoproteins within eight signalling pathways (PI3K, MAPK, β-catenin, STAT, NFκB, ER, cell cycle and DNA damage response), proliferation (phospho-histone H3 and Ki67) and apoptosis (activated caspase 3), in two independent cohorts of ovarian cancers using quantitative immunofluorescence image analysis. Data were analysed by unsupervised and K-means clustering to determine new biologically relevant groups. Expression of markers of the five main pathways deregulated by mutation or copy number changes was different between histological subtypes. Four main clusters with distinct phosphoprotein profiles were identified, which were significantly associated with survival in univariate analysis, and which had distinct patterns of pathway expression reproducible between clinical cohorts. These pathway profiles suggest novel therapeutic regimens for the treatment of ovarian cancer, such as MAPK-inhibition in serous or clear cell carcinomas, or combined inhibition of STAT, NFκB and WNT signalling.

1. Introduction

Survival figures for epithelial ovarian cancer remain poor, with 65% of women dying of their disease within 5 years of diagnosis[1], in spite of often initially good response rates to chemotherapy.[2] This is partly because women with ovarian cancer present with late-stage disease, but also because of a lack of predictive tissue biomarkers coupled with effective therapy in clinical practice, in contrast to the clinical success stories of ER, HER2 and others in breast cancer.[3,4] There is good evidence that platinum–taxane first-line chemotherapy is superior to other chemotherapy regimens for ovarian cancer[2,5–8], but 20–30% of patients do not respond to this therapy. Lower toxicity targeted agents, such as tamoxifen, aromatase inhibitors or trastuzumab (Herceptin) are not routinely used in clinical practice but may have value.[9,10] There is, therefore, an acute need to identify markers of sensitivity to existing cytotoxic agents as well as to identify new 'hits' for targeted

* *Corresponding author:* Tel.: +44 131 537 1763; fax: +44 131 537 3159.
E-mail address: d.faratian@ed.ac.uk (D. Faratian).
0959-8049/$ - see front matter
doi:10.1016/j.ejca.2011.01.014

therapy in ovarian cancer, which could translate into real clinical benefit if currently available therapies can be more precisely targeted to known dysregulated signalling in ovarian cancer.

Recent evidence suggests that distinct molecular subgroups of ovarian cancer exist, both between (Ref. 11) and within (Ref. 12) recognised histopathological subgroups (serous, endometrioid, clear cell and mucinous). This suggests that while histopathology alone provides useful prognostic and predictive information, additional molecular profiling may be able to resolve some of the heterogeneity in response. Molecular classification at protein level may be more informative for therapeutic prediction than gene expression profiling, which so far has only shown benefit in the experimental setting.[13] Although pathway-based gene signatures have been developed for breast cancer[13,14], these are based on well-validated intrinsic subtypes and no agreed classification exists for ovarian cancer. The measurement of proteins is more readily adapted to clinical histopathology labs, which already use immunohistochemistry as a standard molecular technique, facilitating ready transition of proteomic classification to the clinic. Also, drugs are designed to target proteins rather than genes or transcripts. There may be as much as 60% difference between protein and mRNA co-expression[15], and R^2 correlations between mRNA and transcript range between 0 and 0.4 in humans.[16]

The most useful protein targets to measure in order to meet these aims remain open to debate. However, an emerging paradigm within cancer biology, and supported by recent large-scale genotyping and transcriptional profiling studies[17,18], is that the complexity of cancer can be reduced to abnormalities in suppression or activation of only a few pathways, since several different mutations or transcriptional aberrations within the same pathway lead to similar phenotypes.[19] While individual copy gains, losses, or mutation events occur at relatively low frequency in different genes of a given oncogenic signalling pathway, the combined prevalence of pathway level alterations is predicted to be very high (e.g. 90% in RTK/RAS/MAPK pathway in ovarian cancer).[18] We, therefore, reasoned that the expression of proteins or phosphoproteins which would be expected to be deregulated as a result of genomic or non-genomic (i.e. post-translational or signalling-related) changes in the signalling pathway would act as a good surrogate for pathway deregulation, and in one recent paper, a quantitative proteomic approach was used to identify factors associated with platinum response in ovarian cancer, supporting the validity of the proteomic approach.[20] There is emerging data suggesting that measurement of phosphorylated MAPK is more predictive of response to anti-EGFR (epidermal growth factor receptor) therapy than mutation status alone[21] in colorectal cancers, but similar data does not exist in ovarian cancer. Phosphorylation of the serine 473 epitope of AKT provides a measure of the activation state of the PI3K pathway[22], and similar key epitopes are phosphorylated within other pathways driving critical cellular processes such as proliferation, apoptosis, and DNA-damage response (see Table 1).

We sought the most promising pathway candidates from a recent next generation analysis of somatic mutations and copy number changes in ovarian cancer.[18] Five pathways (apoptosis, cell cycle, PI3K/AKT, WNT and RTK/RAS/MAPK) were predicted to be frequently aberrant by either mutation or copy number variation and have functional consequence, and biomarkers representative of the activation of these pathways were sought via a review of the literature and availability of specific antibodies. We also quantified and visualised the activation state of further four growth- or survival-promoting pathways which show minor genetic deregulation (NFκB, ER, components of cell cycle and DNA damage response) in addition to those targets identified by genomic analysis.

We hypothesise that since experimental and clinically used agents already exist which target growth and apoptotic pathways, classification of individual tumours by pathways could result in a tumour specific signature which could guide patient-tailored therapy from a number of readily-available and licensed agents, either alone or in combination. Many of the signalling pathways known to be deregulated in cancer are subject to drug development pipelines, with agents at varying stages of clinical use([23–26] and see clinicaltrials.gov).

The aims of our study were to (1) quantitatively measure the activation state of candidate pathways which are known targets of current or experimental cancer therapeutics by generating a phosphoprotein profile in cancer biopsy tissue, (2) relate this to clinicopathological parameters including histological subtype and stage, and (3) generate new hypotheses for druggable targets in ovarian cancer.

2. Patients and methods

2.1. Study population and design

The study was approved by the Lothian Research Ethics Committee (08/S1101/41). No informed consent (written or verbal) was obtained for use of retrospective tissue samples from the patients within this study, most of whom were deceased, since this was not deemed necessary by the Ethics Committee. The study population consisted of three cohorts of ovarian cancer patients, two of which were independent. The first cohort consisted of 152 formalin fixed, paraffin embedded (FFPE) ovarian tumours treated in the Edinburgh Cancer Centre between 1994 and 2005, as previously described[27], representing a broad range of histological types. The second cohort consisted of 471 FFPE ovarian tumours treated in the Edinburgh Cancer Centre between 1991 and 2006. Finally, 40 frozen ovarian cancer tissues (a subset of cohort 2) were used for validation of phosphoprotein expression. Summary patient characteristics are shown in Table 2. Standard treatment included cytoreductive surgery followed by platinum-based therapy, with or without combination with a taxane. Overall survival was calculated from the date of diagnosis (primary surgery) to the date of death by ovarian cancer, or to the date of last follow-up (censored). Patients who died from disease other than ovarian cancer were censored. Tumours were taken from primary site (not metastatic) and before commencement of chemotherapy.

2.2. Tissue microarray (TMA) construction

The construction of the cohort 1 TMA has already been described[27], and the cohort 2 TMA was similarly constructed.

Table 1 – Pathways studied and the targets used to characterise them.

Target	Supplier	Dilution (AQUA)	Antigen retrieval	Pathway/role in pathway	References
pAKT (Ser 473)	CST (#4060)	1:100	Sodium citrate pH 6.0	PI3-kinase pathway: AKT is a well characterised effector of PI3-kinase, and Ser473 is one of two key activation sites	52,53
pERK (Thr202/Tyr204)	CST (#9101)	1:25	Sodium citrate pH 6.0	MAPK pathway: The p44/42 MAPK (Erk1/2) signalling pathway is a well characterised effector of many cellular processes including proliferation and differentiation, in response to growth factors and cytokines. p44 and p42 are activated through Thr202/Tyr204	54
pER (Ser118)	CST (#2511)	1:500	Sodium citrate pH 6.0	ER pathway: Ser118 resides in the AF1 domain of ER, and when phosphorylated influences DNA binding and recruitment of cofactors, initiating downstream ER-dependent transcription. Activated by MAPK and estradiol, phosphorylation of this residue has been shown to be associated with outcome and response to endocrine therapy by ourselves and others	55–58
pβCatenin (Ser33/37/Thr41)	CST (#9561)	1:25	Sodium citrate pH 6.0	Wnt signalling pathway: Wnt signalling is a critical oncogenic pathway in solid tumours, including ovarian cancer. The Ser33/37/Thr41 sites are critical for GSK-3β mediated phosphorylation and degradation of β-catenin, and therefore low levels of phosphorylation are associated with increased stabilisation of the protein and enhanced WNT signalling. In addition, activation of β-catenin is thought to drive EMT in some experimental systems	59–61
pSTAT3 (Ser727)	CST (#9134)	1:100	Sodium citrate pH 6.0	JAK/STAT signalling pathway: STAT3 is activated in a variety of human cancers, including ovarian cancer. Although tyrosine phosphorylation of STAT3, which is activated by cytokines and EGF, promotes dimerisation and nuclear translocation, phosphorylation of Ser727 is indispensible for maximal transcriptional activity and may therefore act as a better surrogate of pathway activation. In addition, this site is regulated by crosstalk with MAPK and mTOR signalling pathways	62–65
pNFκB (Ser276)	CST (#3037)	1:25	Sodium citrate pH 6.0	NFkB signalling pathway: In addition to controlling inflammatory processes, transcription factor NFκB targets include proliferative and anti-apoptotic genes. Expression of total and phosphorylated forms has recently been recorded in ovarian cancer. Phosphorylation of the p65 subunit at Ser276 enhances activation of the transcription factor through increased interaction with coactivator p300, via PKA and MSK-dependent mechanisms	66–69
pRB (Ser807/811)	CST (#9308)	1:50	Sodium citrate pH 6.0	Cell cycle: pRB negatively regulates cell cycle progression, and interacts with transcription factors to control cell fate. Hyperphosphorylation of pRB occurs during G1/S phase and in particular, Ser807/811 is phosphorylated in a cyclinD1-dependent manner, critical for cell cycle progression	70,71
pH2AX (Ser139)	CST (#9718)	1:50	Sodium citrate pH 6.0	DNA damage response: A very early event in the DNA-damage response, H2A.X is phosphorylated in response to double strand breaks at Ser139, and is required for recruitment of DNA-damage response proteins such as BRCA1	72

pBRCA1 (Ser1524)	CST (#9009)	1:25	Sodium citrate pH 6.0	DNA damage response: BRCA1 is phosphorylated in response to DNA-damage at multiple sites, including Ser1524. This site is also known to be involved in ATR- and claspin-dependent recruitment of BRCA1 to DNA damage, and to initiate caspase-dependent apoptosis	73,74
p-p53 (Ser15)	CST (#9286)	1:100	Sodium citrate pH 6.0	DNA damage response: Although p53 contains multiple phosphorylation sites, Ser15 is a critical DNA-damage induced phosphorylation site and is phosphorylated by ATM, ATR and DNA-PK, and results in decreased interaction with the oncoprotein MDM2 and reduced degradation. It is therefore a candidate biomarker of active DNA-damage and p53 activity	75–78
Ki67	DAKO (M7240)	1:50	Tris–EDTA pH 9.0	Proliferation: Ki67 is a specific marker of proliferation and is expressed in all phases of the cell cycle except G0	79
pHH3	CST (#9701)	1:100	Tris–EDTA pH 9.0	Proliferation: Phosphorylation of the Ser10 residue of histone H3 is a specific marker of chromosome condensation during mitosis	80
Cleaved caspase 3	CST (#9661)	1:200	Sodium citrate pH 6.0	Apoptosis: Caspase 3 is a final effector of apoptosis, and cleavage is required for activation from its inactive zymogen	81

Briefly, four to six replicate TMAs were constructed using established techniques[28], and three replicates were used for analysis within this study. Where primary lesions showed a mixed histological pattern, representative areas of each histological type were targeted, so that all types were adequately represented within the analysis.

2.3. *Immunofluorescence*

Immunofluorescence for phosphoantibodies was performed using methods previously described.[29] Briefly, 4 μm tissue microarray slides were deparaffinized and antigen-retrieved by pressure-cooking according to the reaction conditions shown in Table 1. Endogenous peroxidases were blocked with 2.5% hydrogen peroxide for 15 min and non-specific binding blocked with serum-free protein block for 15 min. Slides were then incubated with primary antibodies diluted in 0.025% PBST for 1 h at room temperature (AE1/AE3 mouse monoclonal cytokeratin antibody with primary antibodies as shown in Table 1). After washing in 0.025% PBST sections were incubated for 1 h at room temperature with secondary antibodies, which included an Alexa 555-conjugated goat anti-mouse antibody diluted 1:100 in 0.1 M TBS, and prediluted goat anti-rabbit antibody conjugated to a horseradish peroxidase-decorated dextran-polymer backbone (EnVision, Dako). Slides were then incubated for 10 min with Cy5-tyramide, which is activated by horseradish peroxidase, to visualise HER2 expression. 4′,6-Diamidino-2-phenylindole (Molecular Probes, Eugene, Ore) was used to stain the nuclear compartment.

2.4. *AQUA automated image analysis*

A detailed description of the AQUA methodology is available elsewhere.[29] Pan-cytokeratin antibody was used to identify infiltrating tumour cells and normal epithelial cells, DAPI-counterstain to identify nuclei, and Cy-5-tyramide detection for target for compartmentalised (tissue and subcellular) analysis of tissue sections. Monochromatic images of each TMA core were captured at 20× objective using an Olympus AX-51 epifluorescence microscope, and high-resolution digital images analysed by the AQUAnalysis software. Briefly, a binary epithelial mask was created from the cytokeratin image of each TMA core. If the epithelium comprised <5% of total core area, the core was excluded from analysis. Similar binary masks were created for cytoplasmic and nuclear compartments based on DAPI staining of nuclei. Phosphoprotein expression was quantified by calculating the Cy5 fluorescent signal intensity on a scale of 0–255 within each image pixel, and the AQUA score generated by dividing the sum of Cy5 signal within the epithelial mask by the area of the cytoplasmic compartment for cytoplasmic proteins or the nuclear compartment for nuclear proteins.

2.5. *Protein Extraction from frozen tissue*

Protein was extracted from 40 ovarian tumours, all of which had pathological confirmation of malignancy. Tumour material (48–250 mg) was placed in an ice-cold flat bottomed soda-glass tube (50 × 12 mm) with 0.3 mL of lysis buffer (50 mM Tris pH 7.5; 5 mM EGTA pH 8.5; 150 mM NaCl supple-

Table 2 – Patient characteristics of the two clinical cohorts used for quantitative immunofluorescence. Overall survival was assessed by Kaplan–Meier analysis with log-rank testing to determine statistical significance (*p*-values shown). MMMT = malignant mixed mesodermal tumour.

	Cohort 1			Cohort 2		
Characteristic	No.	Percent	Log-rank *p*-value	No.	Percent	Log-rank *p*-value
Number of patients	152	100		471	100	
Age			0.018			0.059
Median	61.0	N/A		60.4		
Range	24–90	N/A		27–86		
1st Line chemotherapy regimen			0.36			0.04
Platinum-based	51	33.6		283	60.1	
Platinum and taxane	44	28.9		175	37.2	
Other/none	28	18.4		11	2.3	
Unknown	29	19.1		2	0.4	
Stage			<0.0001			<0.0001
I	29	19.1		47	10.0	
II	20	13.2		56	11.9	
III	52	34.2		271	57.5	
IV	20	13.2		78	16.6	
Unknown	31	20.4		19	4.0	
Histology			0.005			<0.0001
Serous	46	30.3		264	56.1	
Clear cell	31	20.4		24	5.1	
Endometrioid	29	19.1		94	20	
Mixed	23	15.1		61	13	
MMMT	7	4.6		0	0	
Mucinous	14	9.2		14	3.0	
Other	0	0		12	2.5	

mented with protease inhibitors (Roche 11836153001), phosphatase inhibitors (Sigma P2850; P5726) and aprotinin (Sigma A6279)). Samples were homogenised on ice at full power for 2×10 s (with a 30 s interval between bursts to allow the sample to cool down) using a Silverson homogeniser. Resulting homegenates were transferred to pre-cooled microcentrifuge tubes and residual material recovered from the homogeniser with a further 2×0.3 mL of lysis buffer (total pooled volume of each sample = 0.9 mL). Triton X-100 was added to each sample (9 μL/0.9 mL) before centrifuging at 13,000*g* for 30 min at 4 °C after which supernatants were transferred to fresh microcentrifuge tubes. Total protein concentrations were determined by BCA assay and normalised at 2 mg/mL.

2.6. *Reverse phase protein arrays (RPPA)*

Denatured and reduced protein lysates were spotted onto LI-COR (LI-COR Biosciences, Nebraska, USA) nitrocellulose-coated glass slides as previously described.[30,31] Three replicates were spotted per sample in five two-fold dilutions. Slides were hydrated in Li-Cor blocking buffer for 1 h (LI-COR Biosciences, Nebraska, USA), and then incubated with previously optimised primary antibodies overnight at 4 °C in a sealed box containing a damp paper towel (same antibodies as AQUA analysis). The following day slides were washed in PBS/T at room temperature for 5 min (×3) before incubating with far-red fluorescently-labelled secondary antibodies diluted in Li-Cor Odyssey Blocking Buffer (1 μL/2 mL) at room temperature for 45 min with gentle shaking. Slides were then washed in excess PBS/T (×3)/PBS (×3) and allowed to air dry before reading on a Li-Cor Odyssey scanner at 680 and 780 nm and images exported as TIFF files for further analysis.

RPPA analysis was performed using MicroVigene RPPA analysis module (VigeneTech, Carlisle, MA, USA). Spots were quantified by accurate single segmentation, with actual spots signal boundaries determined by the image analysis algorithm. Each spot intensity was quantified by measuring the total pixel intensity of the area of each spot (volume of spot signal pixels), with background subtraction of 2 pixels around each individual spot. The mean of the replicates was used for normalisation and curve fitting. Curve fitting was performed using four parameter logistical non-linear regression using a joint estimation approach ('supercurve method'), with quantification y_0 (intensity of curve) or rsu (relative concentration value) of sample dilution curves used in subsequent analysis.

2.7. *Protein expression analysis and statistics*

AQUA scores were averaged from replicate cores. Protein expression data were analysed in Cluster v2.11 and visualised using Java Treeview, as previously described.[32] Raw AQUA scores were filtered so that >50% of protein expression data was present for each tumour analysed for cohort 1, and >90% for cohort 2. Unsupervised Spearman's average linkage clustering or K-means clustering was performed on filtered AQUA scores which had been log-transformed, and mean-centred to remove bias across TMAs. Overall survival was subsequently assessed by Kaplan–Meier analysis with log-rank testing to determine statistical significance. To assess whether our clusters provided more accurate predictions than standard clinicopathological parameters, we performed

univariate and multivariate analysis using Cox proportional hazards regression models. Comparison of differences in means for pathway expression was performed using the Kruskal–Wallis test, and differences in distribution of histological subtypes and grade per cluster by Chi-squared test. In order to determine the cutpoint value for each of the phosphoproteins for Kaplan–Meier analysis, we utilised X-Tile, which allows determination of an optimal cutpoint while correcting for the use of minimum *P* statistics, as previously described.[33] Two methods of statistical correction for the use of minimal *P* approach were used, the first calculation of a Monte Carlo *P*-value and for the second, the Miller-Siegmund minimal *P* correction.[34] All calculations and analyses were two-tailed where appropriate and done with SPSS 14.0 for Windows (SPSS, Inc., Chicago IL).

3. Results

3.1. Patient characteristics

One-hundred and fifty-two patients in cohort 1 and 471 patients in cohort 2 had sufficient AQUA data after filtering (>50% data present for cohort 1 and >90% data present for cohort 2) for subsequent clustering and survival analysis. Filter thresholds differed between cohorts due to an increased number of lost TMA cores (resulting in missing data) in cohort one, and therefore increased numbers of patients included in the analysis were favoured over completeness of protein expression. Clinicopathological details for these patients is summarised in Table 2. For cohort 1, the median overall survival from diagnosis was 42.9 months (range 0.8–161.0 months) and the 5 year overall survival was 19.0%. For cohort 2, the median overall survival from diagnosis was 32.9 months (range 1.2–211.0 months) and the 5 year overall survival was 30.1%. Cases in cohort 1 were deliberately selected to represent all the main histological types, reflected in the clinical characteristic, while cohort 2 was selected as a more representative ovarian cancer population.

3.2. Pathways driven by genomic aberrations are differentially expressed between histological subtypes of ovarian carcinoma, but unrelated to survival

We sought the most promising pathway candidates from a recent analysis of somatic mutations and copy number changes in ovarian cancer.[18] Five pathways (apoptosis, cell cycle, PI3K/AKT, WNT and RTK/RAS/MAPK) were predicted to be frequently aberrant by either mutation or copy number variation and have functional consequences (Table 3; high combined *q*-score). Quantitative expression of protein surrogates of activation of these pathways (activated caspase 3, Ki67, pAKT(Ser437), pβ-Catenin(Ser33/37Thr41) and pERK(Thr202/Tyr204); Fig. 1, Table 1) showed a wide range of expression, with a 1–2 log-fold range of expression for each of the markers tested. To examine whether pathway aberrations were associated with tumour progression or histogenesis, the expression of pathway markers were compared across different pathological stages and histological types in both tumour cohorts. Only Ki67 expression was associated with increasing pathological stages (Kruskal–Wallis test; $p < 0.0001$) in both cohorts. However, high pERK expression was significantly associated with serous and clear cell carcinomas, and high phospho-β-catenin (associated with destabilisation of β-catenin), low Ki67, and high activated caspase 3 with clear cell carcinomas alone (Fig. 2 and Supplementary Fig. 1). This suggests that certain histological subtypes might be treated with specific targeted therapies, such as serous and clear cell carcinomas with MAPK inhibitors or serous and endometrioid carcinomas with Wnt-pathway inhibitors.

Table 3 – Evaluation of alterations in signalling pathways in ovarian cancer. The combined *q*-score represents a statistical evaluation of both mutation frequency and copy number alteration within each signalling pathway. For detailed explanation, see Ref.[18]

Pathway	Combined *q*-score
APOPTOSIS	16
CELL_CYCLE	16
PI3K/AKT	16
WNT	16
RAS	2.52343
ERK/MAPK	0.71981
JAK/STAT	0.38467
IGF1	0.26454
PDGF	0.15349
DUBs	0.11905
RTK	0.11905
E3	0.11888
EGF signalling	0.05695
PTEN	0.04388
NFkB	0.04296
P38	0.04175
KINASE	0.01009
DNA damage	0
FGF	0
GPCR	0
JNK	0
NOTCH	0

3.3. Aberrant activation of pathways associated with genomic changes is insufficient to stratify patients for prognosis or prediction

We next sought to establish whether aberrant activation of pathways was associated with clinical outcome. Univariate analysis of the five candidate genetic pathways showed no association with overall survival (log-rank test, corrected *p*-value 0.30–0.46). We, therefore, examined combined pathway activation profiles to see whether co-expression of pathways influenced tumour behaviour and clinical outcome. Unsupervised hierarchical clustering revealed two main clusters (Supplementary Figs. 2 and 3) in both cohorts. There were no differences in overall survival between pathway clusters in either cohort of tumours. While there was a suggestion that patients with a profile of pathway activation in cluster one may have a worse outcome when treated with a chemotherapy regimen including a taxane (log rank $p = 0.031$), this was not independent of stage or histology in multivariate analysis. Therefore, while aberrant pathway activation might drive carcinogenetic pathways, the activation status of pathways aber-

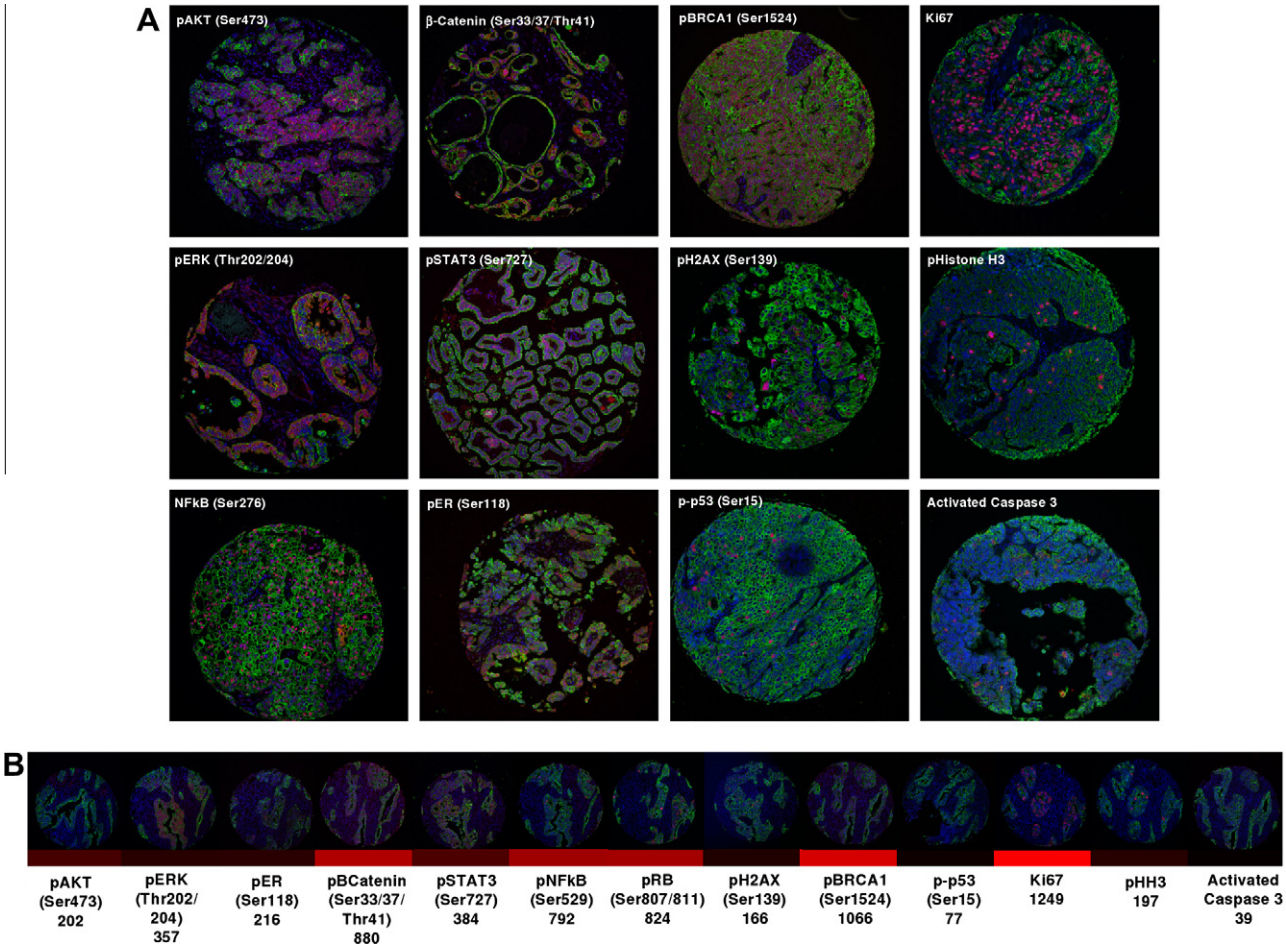

Fig. 1 – AQUA quantitative image analysis. (A) Representative immunofluorescence images of each of the phosphoproteins and pathological markers used within the study. Blue = DAPI nuclear counterstain, green = cytokeratin tumour mask, red = target. (B) Representative staining from an individual case, with corresponding AQUA score represented as both a heatmap and whole integer.

rantly regulated by genomic changes is insufficient to stratify patients for prognosis or prediction.

3.4. *Phosphoprotein profile clusters provide a novel predictive framework for rationalising cancer therapies*

Since there is extensive crosstalk and extra-genomic regulation of signalling pathways, we next sought to establish whether measurement of activation of other key signalling pathways could contribute to histogenesis and prognosis in ovarian cancer. We quantified and visualised the activation state of a further four growth- or survival-promoting pathways which show minor genetic deregulation (NFκB, ER, components of cell cycle, DNA damage response; Supplementary Fig. 4) in addition to those targets already identified by genomic analysis. Representative expression across different cancers is shown in Fig. 1A and in the same cancer in Fig. 1B, in order to illustrate how the AQUA score relates to *in situ* phosphoprotein expression. Phosphoprotein expression was heterogeneous within and between histological subtypes (Supplementary Fig. 5), indicating that similar subtype heterogeneity exists at a functional, phosphoprotein level, to that recently reported for total protein expression in ovarian cancer.[11] These data suggest that crossover exists between morphology and molecular phenotype in ovarian cancer, but that re-classification of tumours by phosphoprotein signature may refine prognostication and prediction by traditional histopathological parameters. In order to determine the value of phosphoprotein profiling compared to traditional histopathological subtyping, we used K-means clustering to organise the tumours on the basis of phosphoprotein expression. Four main clusters were identified (Fig. 3 and Supplementary Fig. 6) in both cohorts of tumours. Baseline assessment of prognosis by univariate log-rank analysis for clinicopathological parameters (Table 2), individual phosphoprotein markers (Supplementary Table 1) and phosphoprotein cluster showed that age, stage, histology, chemotherapy regimen, cluster, pH2A.X, pBRCA1 and pHH3 were all significantly associated with overall survival (Table 1, Fig. 3C and Supplementary Table 1). In univariate analysis, phosphoprotein clusters 3 and 4 differed with respect to overall survival in cohort 2, with cluster 3 having the best prognosis and cluster 4 the worst (log-rank

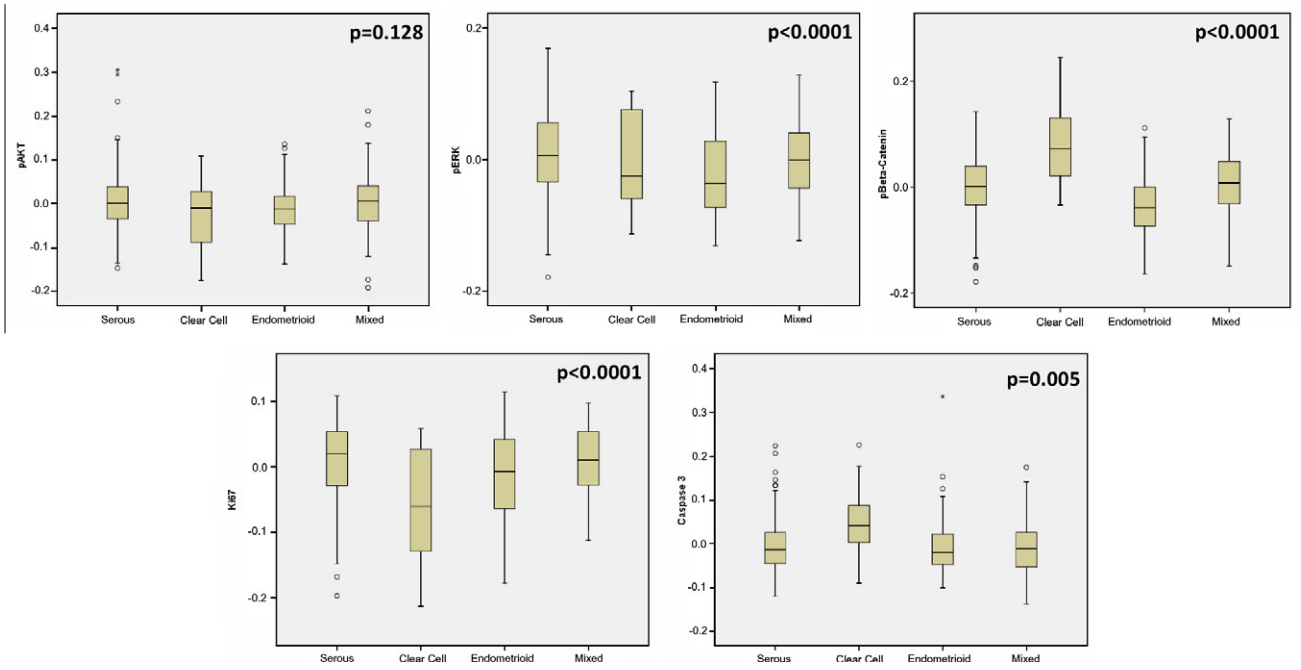

Fig. 2 – Phosphoprotein expression of the five genetic pathway markers between histological subtypes in cohort 2 (*p*-values; Kruskal–Wallis test).

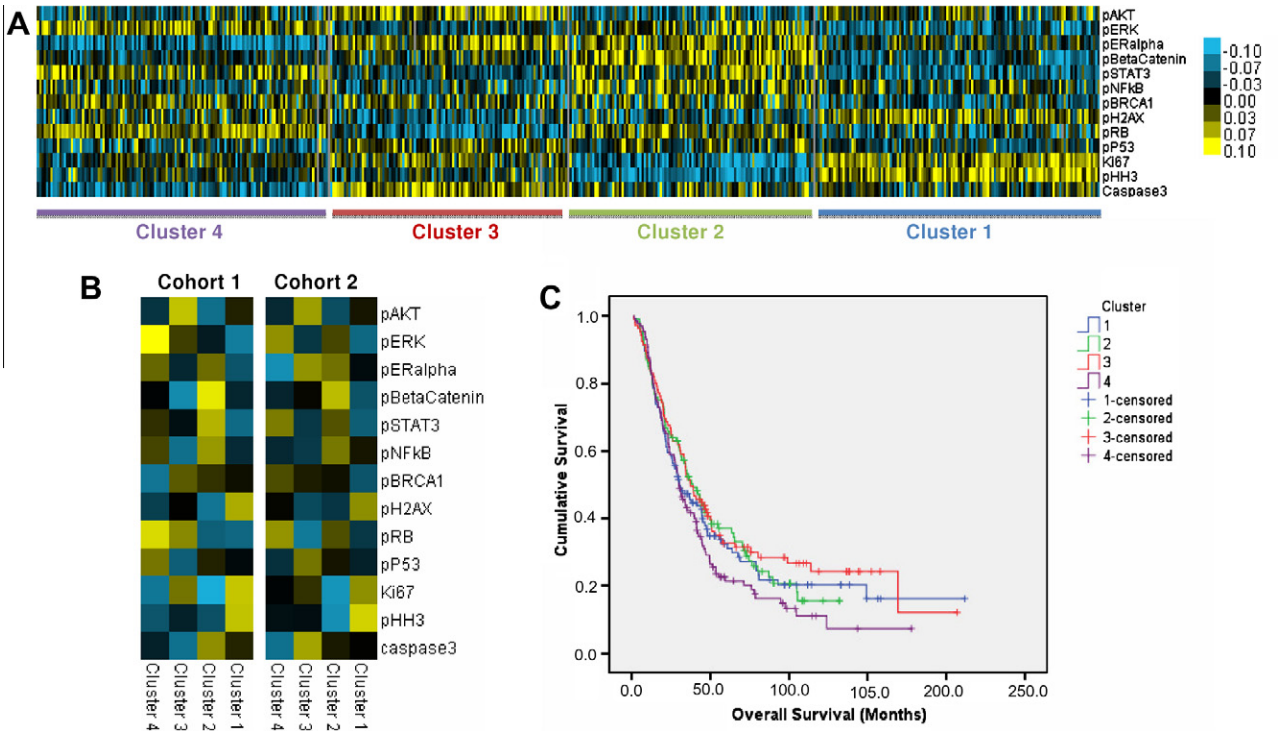

Fig. 3 – K-means clustering of phosphoprotein data (cohort 2 shown here) produces four distinct phosphoprotein clusters (A) with profiles of pathway alteration which are similar between independent clinical cohorts (B). (C) Overall survival according to phosphoprotein cluster (log-rank $p = 0.03$, HR 0.719, 95% CI 0.53–0.96 between clusters 3 and 4).

$p = 0.03$, HR 0.719, 95% CI 0.53–0.96). In cohort 1, there were no significant differences between phosphoprotein clusters, most likely reflecting the small number and unusual distribution of low-grade histological types. However, in multivariate analysis, only stage remained a significant predictor of overall survival in a multivariate Cox regression model (cohort 1;

$p = 0.011$, HR = 1.85 (95% CI 1.06–1.69) and cohort 2; $p = <0.0001$, HR 1.85 (95% CI 1.58–2.10)). There was no association with phosphoprotein cluster and response to chemotherapy.

3.5. *Phosphoprotein pathway analysis suggests novel therapeutic targets in ovarian cancer*

Each of the clusters showed distinct profiles of pathway activation, which were very similar between independent cohorts of samples (Fig. 3B). Cluster 1 tumours were highly proliferative (high Ki67 and phospho-Histone-H3), cluster 2 with consistently high levels of phosphorylation of hormone, growth factor and cytokine-dependent signalling pathways (ER, β-catenin, STAT, NFκB), cluster 3 activation of PI3K and cluster 4 activation of MAPK, STAT high levels of phospho-Rb. In order to ensure that the uncertainty of the stability of phospho-epitopes in formalin-fixed, paraffin-embedded (FFPE) tissue was not unduly biasing the results, we examined a subgroup of these tumours which were available ($n = 40$) as frozen tissue samples for comparison with FFPE tissues. pERK, *p*-β-catenin and pBRCA1 showed significant correlations between RPPA and AQUA (Pearson's correlation coefficient 0.31–0.42; $p < 0.05$). In order to further check that clusters were not biased by preanalytical factors, we measured cytokeratin as a 'housekeeping' protein in the tumour samples. Cytokeratin expression measured by AQUA did not significantly differ between clusters (one-way ANOVA, $p = 0.14$). These profiles suggest that alternative signalling pathways are activated in ovarian cancer and are attractive candidates for personalised medicine using new and existing targeted therapies.

4. Discussion

In this study we clustered human cancers based on the activation state of oncogenic pathways by quantitative phospho-protein expression analysis. We chose ovarian cancer as a model for this approach since the disease has proved resistant to classification using existing approaches such as gene expression array analysis[35,36], although there is mounting evidence to suggest that few well characterised pathways are aberrantly expressed in different histological subtypes.[37] We have shown that while phosphoprotein profiling does show some association with traditional histopathological subtypes, reclassification on the basis of similar phosphoprotein expression by cluster analysis reveals new molecular subgroups. For example, therapeutic targets identified by this approach may be MAPK inhibitors in clear cell carcinomas and combinations of targeted therapies in molecularly classified tumours. Validation in prospective clinical trials, and further investigation *in vitro* and *in vivo* of the therapeutic targets identified herein, are warranted.

Our analysis of upstream signalling pathways has revealed potential new markers which could be targets for new therapies in ovarian cancer. In cluster 3 there is high expression of activated AKT, which is a surrogate for PI3K pathway activation and may be a candidate biomarker for RTK and mTOR inhibitors in breast and other cancers.[38,39] Similar biomarker data for ovarian cancer is lacking. Cluster 2 tumours show a phosphoprotein profile implicating pathways which connect extracellular growth signals from cytokines, growth factors and hormones (β-catenin, STAT, ER; see Supplementary Fig. 4) with cellular growth and survival. Although data exist implicating some of these pathways in ovarian cancer histogenesis, this is the first time that the activation state of these pathways measured by phosphoprotein analysis have been described in clinical samples. Somatic mutations of KRAS[40–42] and CTNNB1 (the gene encoding β-catenin)[43] are seen in mucinous and endometrioid ovarian cancers respectively, and aberrant Wnt, JAK/STAT and MAPK signalling has recently been described in serous ovarian cancers by gene expression analysis.[12] Gene expression profiling studies have similarly shown dominant transcriptional profiles characteristic of specific pathways in histological subtypes. For example, in Tothill et al.[44] the C3 and C6 subtypes identified by transcriptional profiling show overactivation of MAPK and β-catenin pathways and these groups have overrepresentation of low malignant potential and low-grade endometrioid cancers, respectively. These data are not directly comparable with phosphoprotein data, but the phospho-MAPK and β-catenin expression seen in serous cancers is in keeping with the deregulation of these pathways in a proportion of serous cancers, and activated β-catenin is lowest in endometrioid carcinomas, consistent with the C6 subtype, further supporting the validity of the current approach. Likewise, heterogeneous expression of pathways measured by gene expression profiling approaches has also been shown in serous carcinomas[12], but similar to our findings using protein expression, pathway activation alone was a poor prognostic factor in ovarian cancer and combinations of activated pathway profiles yield better prognostic information.[12] In addition, the cohorts used within our study better represent minor histological subtypes, and, therefore, might better represent pathway expression within less well characterised groups, such as clear cell carcinomas. More importantly, each of these pathways represents either existing or novel therapeutic targets, and the pharmacological agents which target them are relatively low toxicity compared with cytotoxic chemotherapies. Good biochemical response rates have been seen in tumours treated with aromatase inhibitors in phase II clinical trials[45–47], and Wnt/β-catenin antagonists have shown promising efficacy *in vitro* and are emerging as new therapeutic targets in cancer.[48] Much less in known about STAT signalling and ovarian cancer therapy, but one study suggests therapeutic efficacy *in vitro* with the JAK inhibitor AG490.[49]

The use of routine archival formalin-fixed, paraffin-embedded tissue samples for phospho-protein detection has potential limitations because of the effect of technical factors (including time-to-fixation and protein cross-linking) on phospho-epitope stability and detection.[50,51] However it is the form of tumour tissue most likely to be available for patients in general clinical and pathological practices. In general, frozen tissues harvested for research have shorter time-to-preservation and are not subject to the cross-linking effects of formalin on proteins. Reassuringly, phosphoprotein expression for available epitopes was found to be similar in both formalin fixed tissues measured by *in situ* protein quantification and frozen tissues measured by RPPA. Expression of the housekeeping protein cytokeratin did not significantly dif-

fer between clusters. These cross-platform analyses in tissue samples handled in very different ways further validates the profiling approach as applicable to samples taken in the routine clinical setting.

In conclusion, this study measures the activation states of a number of pathways by phosphoprotein analysis. This approach offers the opportunity to represent a sufficient amount of the disease complexity with a relatively low volume of data. It not only identifies factors of importance in response prediction to existing chemotherapies, but also several new hypotheses about novel targets and approaches to individualised therapies. These findings will need further validation in both experimental and clinical settings.

Conflict of interest statement

None declared.

Acknowledgements

This work was supported in part by the Scottish Funding Council (Grant Number HR07005; http://www.sfc.ac.uk/), Medical Research Scotland (http://www.medicalresearchscotland.org.uk/), the Cancer Research UK Experimental Cancer Medicine Centre (http://www.cancerresearchuk.org/), and Breakthrough Breast Cancer (http://breakthrough.org.uk/). The funders had no role in study design, data collection and analysis, decision to publish, or preparation of the manuscript.

Appendix A. Supplementary data

Supplementary data associated with this article can be found, in the online version, at doi:10.1016/j.ejca.2011.01.014.

REFERENCES

1. Levi F, Lucchini F, Negri E, Boyle P, La Vecchia C. Cancer mortality in Europe, 1995–1999, and an overview of trends since 1960. *Int J Cancer* 2004;**110**(2):155–69.
2. Cannistra SA. Cancer of the ovary. *N Engl J Med* 2004;**351**(24):2519–29.
3. Payne SJ, Bowen RL, Jones JL, Wells CA. Predictive markers in breast cancer – the present. *Histopathology* 2008;**52**(1):82–90.
4. Faratian D, Clyde RG, Crawford JW, Harrison DJ. Systems pathology-taking molecular pathology into a new dimension. *Nat Rev Clin Oncol* 2009;**6**(8):455–64.
5. International collaborative ovarian neoplasm group. Paclitaxel plus carboplatin versus standard chemotherapy with either single-agent carboplatin or cyclophosphamide, doxorubicin, and cisplatin in women with ovarian cancer: the ICON3 randomised trial. *Lancet* 2002;**360**(9332):505–15.
6. McGuire WP, Hoskins WJ, Brady MF, et al. Cyclophosphamide and cisplatin compared with paclitaxel and cisplatin in patients with stage III and stage IV ovarian cancer. *N Engl J Med* 1996;**334**(1):1–6.
7. Muggia FM, Braly PS, Brady MF, et al. Phase III randomized study of cisplatin versus paclitaxel versus cisplatin and paclitaxel in patients with suboptimal stage III or IV ovarian cancer: a gynecologic oncology group study. *J Clin Oncol* 2000;**18**(1):106–15.
8. Piccart MJ, Bertelsen K, James K, et al. Randomized intergroup trial of cisplatin–paclitaxel versus cisplatin–cyclophosphamide in women with advanced epithelial ovarian cancer: three-year results. *J Natl Cancer Inst* 2000;**92**(9):699–708.
9. Banerjee S, Gore M. The future of targeted therapies in ovarian cancer. *Oncologist* 2009;**14**(7):706–16.
10. Yap TA, Carden CP, Kaye SB. Beyond chemotherapy: targeted therapies in ovarian cancer. *Nat Rev Cancer* 2009;**9**(3):167–81.
11. Kobel M, Kalloger SE, Carrick J, et al. A limited panel of immunomarkers can reliably distinguish between clear cell and high-grade serous carcinoma of the ovary. *Am J Surg Pathol* 2009;**33**(1):14–21.
12. Crijns AP, Fehrmann RS, de Jong S, et al. Survival-related profile, pathways, and transcription factors in ovarian cancer. *PLoS Med* 2009;**6**(2):e24.
13. Bild AH, Yao G, Chang JT, et al. Oncogenic pathway signatures in human cancers as a guide to targeted therapies. Nature 2006;%19;439(7074):353-357.
14. Gatza ML, Lucas JE, Barry WT, et al. A pathway-based classification of human breast cancer. *Proc Natl Acad Sci USA* 2010;**107**(15):6994–9.
15. Wang H, Wang Q, Pape UJ, et al. Systematic investigation of global coordination among mRNA, protein in cellular society. *BMC Genomics* 2010;**11**:364.
16. de Sousa AR, Penalva LO, Marcotte EM, Vogel C. Global signatures of protein and mRNA expression levels. *Mol Biosyst* 2009;**5**(12):1512–26.
17. Wood LD, Parsons DW, Jones S, et al. The genomic landscapes of human breast and colorectal cancers. *Science* 2007;**318**(5853):1108–13.
18. Kan Z, Jaiswal BS, Stinson J, et al. Diverse somatic mutation patterns and pathway alterations in human cancers. *Nature* 2010;**466**(7308):869–73.
19. Vogelstein B, Kinzler KW. Cancer genes and the pathways they control. *Nat Med* 2004;**10**(8):789–99.
20. Carey MS, Agarwal R, Gilks B, et al. Functional proteomic analysis of advanced serous ovarian cancer using reverse phase protein array: TGF-beta pathway signaling indicates response to primary chemotherapy. *Clin Cancer Res* 2010;**16**(10):2852–60.
21. Perkins G, Lievre A, Ramacci C, et al. Additional value of EGFR downstream signaling phosphoprotein expression to KRAS status for response to anti-EGFR antibodies in colorectal cancer. *Int J Cancer* 2010;**127**(6):1321–31.
22. McCubrey JA, Steelman LS, Abrams SL, et al. Roles of the RAF/MEK/ERK and PI3K/PTEN/AKT pathways in malignant transformation and drug resistance. *Adv Enzyme Regul* 2006;**46**:249–79. Epub;%2006 Jul 18.
23. Baud V, Karin M. Is NF-kappaB a good target for cancer therapy? Hopes and pitfalls. *Nat Rev Drug Discov* 2009;**8**(1):33–40.
24. Yue P, Turkson J. Targeting STAT3 in cancer: how successful are we? *Expert Opin Investig Drugs* 2009;**18**(1):45–56.
25. Wallin JJ, Guan J, Prior WW, et al. Nuclear phospho-Akt increase predicts synergy of PI3K inhibition and doxorubicin in breast and ovarian cancer. *Sci Transl Med* 2010;**2**(48):48ra66.
26. Pratilas CA, Solit DB. Targeting the mitogen-activated protein kinase pathway: physiological feedback and drug response. *Clin Cancer Res* 2010;**16**(13):3329–34.
27. Graham AD, Faratian D, Rae F, Thomas JS. Tissue microarray technology in the routine assessment of HER-2 status in invasive breast cancer: a prospective study of the use of immunohistochemistry and fluorescence in situ hybridization. *Histopathology* 2008;**52**(7):847–55.

28. Kononen J, Bubendorf L, Kallioniemi A, et al. Tissue microarrays for high-throughput molecular profiling of tumor specimens. *Nat Med* 1998;**4**(7):844–7.
29. Camp RL, Chung GG, Rimm DL. Automated subcellular localization and quantification of protein expression in tissue microarrays. *Nat Med* 2002;**8**(11):1323–7.
30. Spurrier B, Ramalingam S, Nishizuka S. Reverse-phase protein lysate microarrays for cell signaling analysis. *Nat Protoc* 2008;**3**(11):1796–808.
31. Faratian D, Goltsov A, Lebedeva G, et al. Systems biology reveals new strategies for personalizing cancer medicine and confirms the role of PTEN in resistance to trastuzumab. *Cancer Res* 2009;**69**(16):6713–20.
32. Eisen MB, Spellman PT, Brown PO, Botstein D. Cluster analysis and display of genome-wide expression patterns. *Proc Natl Acad Sci USA* 1998;**95**(25):14863–8.
33. Camp RL, Dolled-Filhart M, Rimm DL. X-tile: a new bio-informatics tool for biomarker assessment and outcome-based cut-point optimization. *Clin Cancer Res* 2004;**10**(21):7252–9.
34. Altman DG, Lausen B, Sauerbrei W, Schumacher M. Dangers of using "optimal" cutpoints in the evaluation of prognostic factors. *J Natl Cancer Inst* 1994;**86**(11):829–35.
35. Israeli O, Goldring-Aviram A, Rienstein S, et al. In silico chromosomal clustering of genes displaying altered expression patterns in ovarian cancer. *Cancer Genet Cytogenet* 2005;**160**(1):35–42.
36. Lawrenson K, Gayther SA. Ovarian cancer: a clinical challenge that needs some basic answers. *PLoS Med* 2009;**6**(2):e25.
37. Willner J, Wurz K, Allison KH, et al. Alternate molecular genetic pathways in ovarian carcinomas of common histological types. *Hum Pathol* 2007;**38**(4):607–13.
38. Marinov M, Ziogas A, Pardo OE, et al. AKT/mTOR pathway activation and BCL-2 family proteins modulate the sensitivity of human small cell lung cancer cells to RAD001. *Clin Cancer Res* 2009;**15**(4):1277–87.
39. Berns K, Horlings HM, Hennessy BT, et al. A functional genetic approach identifies the PI3K pathway as a major determinant of trastuzumab resistance in breast cancer. *Cancer Cell* 2007;**12**(4):395–402.
40. Cuatrecasas M, Villanueva A, Matias-Guiu X, Prat J. K-ras mutations in mucinous ovarian tumors: a clinicopathologic and molecular study of 95 cases. *Cancer* 1997;**79**(8):1581–6.
41. Enomoto T, Weghorst CM, Inoue M, Tanizawa O, Rice JM. K-ras activation occurs frequently in mucinous adenocarcinomas and rarely in other common epithelial tumors of the human ovary. *Am J Pathol* 1991;**139**(4):777–85.
42. Ichikawa Y, Nishida M, Suzuki H, et al. Mutation of K-ras protooncogene is associated with histological subtypes in human mucinous ovarian tumors. *Cancer Res* 1994;**54**(1):33–5.
43. Gamallo C, Palacios J, Moreno G, et al. Beta-catenin expression pattern in stage I and II ovarian carcinomas: relationship with beta-catenin gene mutations, clinicopathological features, and clinical outcome. *Am J Pathol* 1999;**155**(2):527–36.
44. Tothill RW, Tinker AV, George J, et al. Novel molecular subtypes of serous and endometrioid ovarian cancer linked to clinical outcome. *Clin Cancer Res* 2008;**14**(16):5198–208.
45. Langdon SP, Smyth JF. Hormone therapy for epithelial ovarian cancer. *Curr Opin Oncol* 2008;**20**(5):548–53.
46. Walker G, MacLeod K, Williams AR, et al. Estrogen-regulated gene expression predicts response to endocrine therapy in patients with ovarian cancer. *Gynecol Oncol* 2007;**106**(3):461–8.
47. Smyth JF, Gourley C, Walker G, et al. Antiestrogen therapy is active in selected ovarian cancer cases: the use of letrozole in estrogen receptor-positive patients. *Clin Cancer Res* 2007;**13**(12):3617–22.
48. Bafico A, Liu G, Goldin L, Harris V, Aaronson SA. An autocrine mechanism for constitutive Wnt pathway activation in human cancer cells. *Cancer cell* 2004;**6**(5):497–506.
49. Roberts D, Schick J, Conway S, et al. Identification of genes associated with platinum drug sensitivity and resistance in human ovarian cancer cells. *Br J Cancer* 2005;**92**(6):1149–58.
50. Baker AF, Dragovich T, Ihle NT, et al. Stability of phosphoprotein as a biological marker of tumor signaling. *Clin Cancer Res* 2005;**11**(12):4338–40.
51. Espina V, Edmiston KH, Heiby M, et al. A portrait of tissue phosphoprotein stability in the clinical tissue procurement process. *Mol Cell Proteomics* 2008;**7**(10):1998–2018.
52. Burgering BM, Coffer PJ. Protein kinase B (c-Akt) in phosphatidylinositol-3-OH kinase signal transduction. *Nature* 1995;**376**(6541):599–602.
53. Scheid MP, Marignani PA, Woodgett JR. Multiple phosphoinositide 3-kinase-dependent steps in activation of protein kinase B. *Mol Cell Biol* 2002;**22**(17):6247–60.
54. Roux PP, Blenis J. ERK and p38 MAPK-activated protein kinases: a family of protein kinases with diverse biological functions. *Microbiol Mol Biol Rev* 2004;**68**(2):320–44.
55. Lannigan DA. Estrogen receptor phosphorylation. *Steroids* 2003;**68**(1):1–9.
56. Kuske B, Naughton C, Moore K, et al. Endocrine therapy resistance can be associated with high estrogen receptor alpha (ERalpha) expression and reduced ERalpha phosphorylation in breast cancer models. *Endocr Relat Cancer* 2006;**13**(4):1121–33.
57. Zoubir M, Mathieu MC, Mazouni C, et al. Modulation of ER phosphorylation on serine 118 by endocrine therapy: a new surrogate marker for efficacy. *Ann Oncol* 2008;**19**(8):1402–6.
58. Yamashita H, Nishio M, Toyama T, et al. Low phosphorylation of estrogen receptor alpha (ERalpha) serine 118 and high phosphorylation of ERalpha serine 167 improve survival in ER-positive breast cancer. *Endocr Relat Cancer* 2008;**15**(3):755–63.
59. Yost C, Torres M, Miller JR, et al. The axis-inducing activity, stability, and subcellular distribution of beta-catenin is regulated in Xenopus embryos by glycogen synthase kinase 3. *Genes Dev* 1996;**10**(12):1443–54.
60. Morin PJ, Sparks AB, Korinek V, et al. Activation of beta-catenin-Tcf signaling in colon cancer by mutations in beta-catenin or APC. *Science* 1997;**275**(5307):1787–90.
61. Stemmer V, de Craene B, Berx G, Behrens J. Snail promotes Wnt target gene expression and interacts with beta-catenin. *Oncogene* 2008;**27**(37):5075–80.
62. Lufei C, Koh TH, Uchida T, Cao X. Pin1 is required for the Ser727 phosphorylation-dependent Stat3 activity. *Oncogene* 2007;**26**(55):7656–64.
63. Wen Z, Zhong Z, Darnell Jr JE. Maximal activation of transcription by Stat1 and Stat3 requires both tyrosine and serine phosphorylation. *Cell* 1995;**82**(2):241–50.
64. Bromberg JF, Wrzeszczynska MH, Devgan G, et al. Stat3 as an oncogene. *Cell* 1999;**98**(3):295–303.
65. Yokogami K, Wakisaka S, Avruch J, Reeves SA. Serine phosphorylation and maximal activation of STAT3 during CNTF signaling is mediated by the rapamycin target mTOR. *Curr Biol* 2000;**10**(1):47–50.
66. Zhong H, SuYang H, Erdjument-Bromage H, Tempst P, Ghosh S. The transcriptional activity of NF-kappaB is regulated by the IkappaB-associated PKAc subunit through a cyclic AMP-independent mechanism. *Cell* 1997;**89**(3):413–24.
67. Zhong H, Voll RE, Ghosh S. Phosphorylation of NF-kappa B p65 by PKA stimulates transcriptional activity by promoting a novel bivalent interaction with the coactivator CBP/p300. *Mol Cell* 1998;**1**(5):661–71.
68. Vermeulen L, De Wilde G, Van Damme P, Vanden Berghe W, Haegeman G. Transcriptional activation of the NF-kappaB p65

subunit by mitogen- and stress-activated protein kinase-1 (MSK1). *EMBO J* 2003;**22**(6):1313–24.
69. Darb-Esfahani S, Sinn BV, Weichert W, et al. Expression of classical NF-kappaB pathway effectors in human ovarian carcinoma. *Histopathology* 2010;**56**(6):727–39.
70. Paternot S, Arsenijevic T, Coulonval K, et al. Distinct specificities of pRb phosphorylation by CDK4 activated by cyclin D1 or cyclin D3: differential involvement in the distinct mitogenic modes of thyroid epithelial cells. *Cell Cycle* 2006;**5**(1):61–70.
71. Sherr CJ. Cancer cell cycles. *Science* 1996;**274**(5293):1672–7.
72. Yuan J, Adamski R, Chen J. Focus on histone variant H2AX: to be or not to be. *FEBS Lett* 2010;**584**(17):3717–24.
73. Martin SA, Ouchi T. BRCA1 phosphorylation regulates caspase-3 activation in UV-induced apoptosis. *Cancer Res* 2005;**65**(23):10657–62.
74. Lin SY, Li K, Stewart GS, Elledge SJ. Human Claspin works with BRCA1 to both positively and negatively regulate cell proliferation. *Proc Natl Acad Sci USA* 2004;**101**(17):6484–9.
75. Shieh SY, Ikeda M, Taya Y, Prives C. DNA damage-induced phosphorylation of p53 alleviates inhibition by MDM2. *Cell* 1997;**91**(3):325–34.
76. Meek DW. Post-translational modification of p53. *Semin Cancer Biol* 1994;**5**(3):203–10.
77. Appella E, Anderson CW. Post-translational modifications and activation of p53 by genotoxic stresses. *Eur J Biochem* 2001;**268**(10):2764–72.
78. Milczarek GJ, Martinez J, Bowden GT. P53 Phosphorylation: biochemical and functional consequences. *Life Sci* 1997;**60**(1):1–11.
79. Gerdes J, Lemke H, Baisch H, et al. Cell cycle analysis of a cell proliferation-associated human nuclear antigen defined by the monoclonal antibody Ki-67. *J Immunol* 1984;**133**(4):1710–5.
80. Hendzel MJ, Wei Y, Mancini MA, et al. Mitosis-specific phosphorylation of histone H3 initiates primarily within pericentromeric heterochromatin during G2 and spreads in an ordered fashion coincident with mitotic chromosome condensation. *Chromosoma* 1997;**106**(6):348–60.
81. Nicholson DW, Ali A, Thornberry NA, et al. Identification and inhibition of the ICE/CED-3 protease necessary for mammalian apoptosis. *Nature* 1995;**376**(6535):37–43.